Research Square

Preprints are preliminary reports that have not undergone peer review.
They should not be considered conclusive, used to inform clinical practice,
or referenced by the media as validated information.

Mechanisms involved in the positive effects of high zinc on growth of Sedum alfredii

Yuxiao Gao (22114159@zju.edu.cn)
Zhejiang University
Haiyue Yu
Haizhong Lin
Lingli Lu

Research Article

Keywords: Sedum alfredii Hance, Hyperaccumulation, Zinc growth-promoting mechanism, Transcriptome.

Posted Date: October 19th, 2023

DOI: https://doi.org/10.21203/rs.3.rs-3444862/v1

License: This work is licensed under a Creative Commons Attribution 4.0 International License.
Read Full License

Abstract

Background and Aims: Zinc (Zn) is an essential micronutrient for plant growth, and excessive Zn in the soil can inhibit normal plant growth, adversely affecting plant health. *Sedum alfredii* Hance, a native Zn/Cd hyperaccumulator plant species in China, has strong tolerance and ability to accumulate heavy metals. Previous studies have reported that Zn may have a positive effect on *S. alfredii* growth, rather than causing toxicity. Thus, exploring the growth-promoting mechanisms of high Zn concentrations on *S. alfredii* may provide a theoretical reference for phytoremediation technologies.

Methods: In this study, the hyperaccumulating ecotype (HE) and non-hyperaccumulating ecotype (NHE) of *S. alfredii* as research subjects, we used metabolomics, metabolomics, and transcriptomics techniques to explore.

Results: At 250 μM Zn, HE root biomass and Zn concentration in roots increased, while being reduced in NHE. Nano-XRF analysis showed that Zn was located in the cortical intercellular space in HE roots, whereas Zn was scattered in the root cells in NHE. The content of auxin in HE roots was increased by 1.26 times and the auxin oxidase activity decreased by 2.94 times after exposure to 100 μM Zn for 12 h, while NHE exhibited the opposite trend. Transcriptomic results showed that HE up-regulated genes were related to carbohydrate metabolism, nitrogen metabolism, carbon fixation, and tryptophan biosynthesis; down-regulated genes were related to lipid metabolism and linoleic acid metabolism.

Conclusion: We further screened key gene resources, laying a foundation for the molecular mechanism underlying the positive effect of high Zn concentration on HE growth.

Introduction

Zinc (Zn) is an essential micronutrient for plants and is closely related to plant growth and development (Broadley et al. 2007). Zinc affects plant growth by altering root dry weight, shoot biomass, and leaf area (Azhar et al. 2020). It participates in plant photosynthesis by influencing net photosynthesis, stomatal conductance, photosystem efficiency, and chloroplast integrity (Pavia et al. 2019). Moreover, Zn influences the activities of a variety of enzymes and plays an important role in hydrolysis, redox, and protein synthesis processes (Noreen et al. 2021). It also changes plant cell structure by affecting cell elongation, stomatal density, and plasma membrane integrity (Tavallali 2017). Plant roots play a pivotal role in the uptake of Zn from the soil. Lateral roots rely on expanding the root-soil contact area to increase nutrient uptake for plant growth. Studies have shown that the apparent contribution of lateral roots to Zn uptake was 49.7–57.4% in hydroponic experiments (Liu et al. 2013). Therefore, it is crucial to explore the mechanisms by which Zn affects the growth of lateral roots to further understand the growth-promoting effects of Zn on plants. Recent studies have shown that Zn affects plant root growth through its effects on auxin biosynthesis, transportation, and metabolism (Wang et al. 2021). The auxin (indole acetic acid, IAA) biosynthetic pathway mostly relies on tryptophan, which is generally considered the precursor of IAA

biosynthesis (Wang et al. 2012). As Zn is an essential component of tryptophan synthase, it is an indispensable element for auxin biosynthesis in plants.

Excessive Zn in the soil can inhibit normal plant growth (Edelstein & Ben-Hur 2018). On the one hand, Zn toxicity inhibits the growth of plant roots, which first manifests as a harmful root tip, leading to inhibition of the growth of the entire root system. This toxicity can cause oxidative stress in the root system, destroy the biofilm system of plant cells, and affect the normal physiological functions of cells (dos Santos et al. 2020). Zinc toxicity also causes vacuolization of plant root meristem cells, granular deposition in vacuoles, cell wall thickening, mitochondrial matrix concentration, cytoplasmic thinning, and endoplasmic reticulum enlargement (Glinska et al. 2016). On the other hand, excessive Zn can also inhibit photosynthesis in plants, which is manifested as weakened photosynthesis, reduced transpiration, and leaf chlorosis (Anjum et al. 2015). For Zn detoxification, plants fix metal ions via chelation (Gong & Shen 2010). *Cardaminopsis halleri* can transfer Zn to vacuoles and achieve detoxification by compartmentalization (Neumann & zur Nieden 2001). Zinc stress can affect the activity of plant antioxidant enzymes (APX, SOD, POD, and CAT) and the content of antioxidants (AsA and GSH), scavenging oxygen free radicals to protect cells from damage (Ding et al. 2005; Sun et al. 2008; Wang et al. 2009). Plants secrete soluble sugars, soluble proteins, proline, and other osmotic adjustment substances to maintain the water balance of cells and tissues, stabilize the structure of biological macromolecules, and maintain normal cell metabolism (Guo et al. 2009; Mehta & Gaur 1999; Xu et al. 2006). However, hyperaccumulators, special plant species that differ from others, can grow normally under high Zn conditions. For instance, *Noccaea caerulescens* can accumulate 21,000 mg/kg of Zn under natural conditions (Baker, et al., 1994), and Zn mainly accumulates in the leaves of *N. caerulescens* under hydroponic conditions. Its transport coefficient is 2–4.1 under 200–500 μM Zn treatment conditions (Dinh, et al., 2015). Clearly, the effects of high Zn on hyperaccumulators and non-hyperaccumulators are different, and the mechanism of hyperaccumulation requires further study.

Sedum alfredii Hance is a native Zn/cadmium (Cd) hyperaccumulator plant species in China. It has a strong tolerance and ability to accumulate heavy metals such as Zn and Cd (Yang et al. 2004). In nutrient solution, the highest Zn concentrations in the leaves and stems of the hyperaccumulating ecotype (HE) of *S. alfredii* were 17,300 and 21,945 mg/kg, respectively, which were 16 and 18 times greater than those of the non-hyperaccumulating ecotype (NHE). The hyperaccumulation of Zn in plants changes their root structure to promote the formation of side roots (Balafrej et al., 2020). It has been observed in previous studies that Zn may increase the biomass, root length, surface area, and volume of *S. alfredii* under Cd stress (Ye et al. 2003). However, preliminary studies on *S. alfredii* have focused on Zn accumulation, absorption, and transport characteristics (Li et al. 2009; Li et al. 2005), and few studies have focused on the phenomenon that appropriate concentrations of Zn may promote the growth of hyperaccumulator plants. Therefore, the specific effect of high concentrations of Zn on the growth of *S. alfredii* and its mechanism of action remain unclear.

Our study used two ecotypes of *S. alfredii* as research objects and applied metallomics technologies to study the growth-promoting effect of high Zn concentrations on *S. alfredii* and transcriptomics

technologies to discover the functional genes that may play key roles. This study provides a theoretical reference for the optimization of phytoremediation technology for heavy metal-contaminated soil, and can also provide a new perspective for interpreting the theory of plant Zn nutrition.

Materials and Methods

Plant materials and pre-cultivation

The hyperaccumulating ecotype (HE) of *Sedum alfredii* Hance was obtained from an old Pb/Zn mined area in Quzhou, Zhejiang Province, China, and the non-hyperaccumulating ecotype (NHE) of *S. alfredii* was obtained from a tea plantation in Hangzhou, Zhejiang Province, China. Plants were cultivated in non-contaminated soil for several generations to minimize the internal metal content. After germination, healthy and equal-sized seedlings were selected and transferred to pure water for 1 week, then subjected to ¼ and ½ strength nutrient solution for 4 days successively, and then pre-cultured in full-strength nutrient solution. The nutrient solution was prepared as described previously (Tian et al. 2011). The pH of the nutrient solution was adjusted to 5.8 daily using 0.1 M HCl or 0.1 M NaOH, and the nutrient solution was renewed every 3 days. Plants were cultivated in an artificial climate room with natural light for 16 h per day, day/night temperature of 25/23°C and humidity of 55–65% (Lu et al. 2008).

Plant growth and biomass

One-week-old seedlings of the two *S. alfredii* ecotypes were treated with different Zn concentrations (0.5, 5, 100, or 250 μM) for 7 days. Zn^{2+} was added as $ZnSO_4$. Each treatment was replicated six times, with seven individual plants per pot. Plant roots were photographed using a root scanner (Epson Perfection V850 Pro, Japan). Lateral roots were photographed using a camera (Andor NEO-5.5-CL3, EU) connected to an optical stereoscopic microscope (Nikon ECLIPSE Ni-E, Japan). The plants were immersed in 20 mM Na_2-EDTA for 15 min and rinsed three times with deionized water. The plants were separated into roots, stems, and leaves, or roots and shoots, and the fresh weight (biomass) of each sample was recorded.

Element analysis

Four-week-old seedlings of the two *S. alfredii* ecotypes were treated with different Zn levels (0.5, 5, 100, or 250 μM) for 7 days. Three plants from each culture vessel were treated as one replicate and each treatment had five replicates. The harvested plants were oven dried at 65°C for 72 h to a constant weight, and dry weight was recorded. Dry plant samples from each treatment were digested at 180°C with 5 mL HNO_3 (1.0 M) and 1 mL H_2O_2 (1.0 M) until the solution was clear and transparent. The cooled digestion solution was diluted to an appropriate volume using ultrapure water, and filtered through a 0.22-μm-pore filter membrane. Zn and Cd contents were determined using an atomic absorption spectrophotometer (SP-3530AA, Shanghai Spectrum, Shanghai, China).

Root length and number of lateral roots

Lateral roots of seedlings of two *S. alfredii* ecotypes pre-cultured for 7 days were quantified using a microscope and photographed using a root scanner. The root systems were observed using a WinRHIZO 2017 Pro to measure various indices. ImageJ was used to evaluate and analyze the lengths of the lateral roots, mature lateral root zone, new lateral root zone, lateral root primordium zone, no lateral root zone, new germination lateral root zone, lateral root apex, and adventitious root apex.

The boundaries of each division in the root were as follows: from the tip of the root apex to the first mature root hair (no change in length) measured as the root apex length; to the first lateral root primordium measured as the lateral root primordium area and the non-lateral root area; when the first lateral root appeared was the boundary between the new lateral root zone and the lateral root primordium zone; and the first mature lateral root (lateral root with mature root hairs) measured as the boundary between the mature lateral root zone and the new lateral root zone.

Determination of auxin and cytokinin content

Four-week-old seedlings of the two *S. alfredii* ecotypes were treated with 5 μM $ZnSO_4$ (control) or 100 μM $ZnSO_4$ for 0 h, 1 h, 3 h, 6 h, 12 h, 24 h, 3 d and 7 d, respectively. Three plants in each culture vessel were treated as one replicate, and each treatment and time point had three replicates. The fresh root samples were washed and ground in liquid nitrogen. The powder was extracted in 1 mL of pre-cooled (-20°C) extractant (methanol:water:formic acid = 15:4:1, v:v, containing 10 mg/L BHT, w/v), and stored at -20°C overnight. The extract was centrifuged at 4°C at 15,000 g for 30 min, the supernatant was reserved, the residue was extracted and centrifuged again, and the supernatants from two centrifugations were mixed and blown dry. Phytohormones were dissolved in 300 μL of 1 M methanol. Auxin and cytokinin contents were determined using a Plant Auxin ELISA and Plant Cytokinin ELISA test kit (Shenzhen Zike Biotechnology Co., Ltd.), respectively, according to the manufacturer's instructions. Absorbance was measured using a microplate reader.

Determination of auxin oxidase activity

Auxin oxidase activity was determined using an indole acetate oxidase activity determination kit (Sinobestbio) according to the manufacturer's instructions. Fresh root samples were washed and ground in liquid nitrogen, and the extract was added. The extract was centrifuged at 4°C at 8000 g for 10 min. Then the supernatant was mixed with reagents and incubated at 30°C. The absorbance (OD) was measured at 530 nm using a microplate reader.

Element distribution characteristics analysis

Four-week-old seedlings of the two *S. alfredii* ecotypes were treated with 5 (control) or 250 μM $ZnSO_4$ for 7 days. High-pressure freezing (HPF) followed by freeze substitution (FS) was used to maintain the ultrastructure of the root tip and lateral root samples. The nano-XRF samples were cut to a length of 2 mm and placed in a high-pressure freezer (HPM-100; EM ICE, Leica, Germany) for freezing and fixing. The fixed samples were kept in 1% osmium acid-acetone solution at -90°C, -60°C, and − 30°C for 8 hours to fully fix the components. Then the samples were reserved at 0°C for 1 h and washed with pure acetone

twice for 15 min each time. Resin was used to infiltrate, embed, and polymerize the samples to obtain embedding blocks. The embedding block was ultra-thin sectioned on a microtome (EM UC7, Leica, Germany) at a thickness of 3 μm. Nano-XRF was performed in a helium atmosphere on an Advanced Photon Source (APS) 2-ID-E hard X-ray microprobe beamline at the Argonne National Laboratory in the United States (Xie et al. 2020). The resulting element maps were visualized and analyzed using MAPS software.

Transcriptome analysis

RNA extraction, library establishment, and Illumina sequencing

After 4 weeks of pre-culturing, HE *S. alfredii* were treated with 5 (control) or 100 μM $ZnSO_4$ for 24 h, and each treatment had three replicates. Total RNA was extracted from HE roots using TRIzol reagent (Invitrogen, CA, USA), and RNA integrity was assessed using a Bioanalyzer 2100 system (Agilent Technologies, CA, USA). A sequencing library was generated using the NEBNext® Ultra™ RNA Library Prep Kit for Illumina® (NEB, USA). After cluster generation, the library preparations were sequenced on the Illumina Hiseq™ platform and 150 bp paired-end reads were generated.

Data assembly and annotation

Raw data were first processed using in-house Perl scripts, including the removal of reads containing adapters, reads containing poly-N, and low-quality reads. All the downstream analyses were based on high-quality clean data. Transcriptome assembly was accomplished based on paired-end reads using Trinity software, with min_kmer_cov set to 2 by default, and all other parameters set to default. Corset software was used to perform hierarchical clustering. The longest cluster sequence was used for subsequent analyses. Gene function was annotated based on the Nr (NCBI non-redundant protein sequences), Nt (NCBI non-redundant nucleotide sequences), Pfam (protein family), KOG (eukaryotic Ortholog Groups), Swiss-Prot (a manually annotated and reviewed protein sequence database), KEGG (Kyoto Encyclopedia of Genes and Genomes), and GO (Gene Ontology) databases. The read counts were transferred to FPKM at the gene expression level. Differential expression analysis was performed using the DESeq R package (version 1.10.1). Individual genes were considered differentially expressed genes (DEGs) when $P < 0.05$. KOBAS software was used to test the statistical enrichment of DEGs in the KEGG pathways.

Statistical analysis

All statistical analyses were conducted using SPSS v22.0 software. The mean and standard deviation of each group of data were calculated and analyzed using one-way analysis of variance (ANOVA). Significant differences were indicated by Fisher's least significant difference (LSD) test and Duncan's multiple range test at the $P < 0.05$ level. Drawing was performed using Origin 8.0 software.

Results

Effects of Zn on plant growth and biomass

After one week of treatment at different Zn levels, the biomass of HE roots increased by 80.2% (100 μM Zn) and 152.7% (250 μM Zn) compared to the control (5 μM Zn). High-Zn (250 μM Zn) treatment also markedly increased the biomass of HE stems by 23.3%, implying that increasing the Zn concentration significantly promoted the growth of HE. However, no significant effects in the biomass of HE roots, stems, and leaves were observed under low-Zn (0.5 μM Zn) treatment (Fig. 1c). In contrast, excess Zn significantly inhibited NHE plant growth, with 250 μM Zn exposure decreasing root biomass by 44.7% compared to the control values. There was no significant effect on the biomass of NHE stems and leaves (Fig. 1d).

Effects of Zn on roots and lateral roots

At the 100 and 250 μM Zn levels, increases were observed in the total HE root length of 54.2% and 103.6%, root surface area of 51.2% and 129.7%, and root volume of 108% and 207%, respectively. The low-Zn treatment had no significant effect on HE roots compared with the control (Fig. 2c–e). However, 250 μM Zn treatment significantly reduced the total NHE root length, surface area, and volume of roots by 69.6%, 70.3%, and 40.1%, respectively. No significant differences in average root diameter were observed between HE and NHE at any Zn level (Fig. 2f). In general, external Zn application promotes HE root growth by increasing the total length, surface area, and volume of the root system. In contrast, Zn deficiency and excess inhibited the growth of NHE roots.

Both ecotypes responded differently to Zn exposure in terms of lateral root development (Fig. 3a–b). At 250 μM Zn treatment, the total number of HE lateral roots significantly increased by 1.49 times, while those of NHE were significantly reduced by 40.1% compared with the control. The average HE lateral root length increased by 58.5% (100 μM Zn) and 178.6% (250 μM Zn) compared with that of the control (Fig. 3c–d). However, low-Zn treatment had no significant effect on the length of HE lateral roots. The lateral root length of NHE showed no obvious response to Zn exposure. In addition, during one-week treatments with different Zn levels, the germination rate of HE lateral roots showed an increasing trend, whereas a decreasing trend was observed in NHE lateral roots (Fig. 3e–f).

To further investigate the effect of Zn on lateral root development, lateral roots were zoned according to germination status (Fig. 4a). In general, high-Zn treatment significantly increased the length of the lateral root maturation zone, new lateral root zone, lateral root tip, and adventitious root tip in HE, whereas they significantly decreased in NHE. Zn treatment had no effect on the length of the HE lateral root zone, whereas that of the NHE decreased (Fig. 4f–k). The length of the root tip depends on the lengths of the elongation and maturation zones. High-Zn treatment increased the length of the HE lateral root tip, but inhibited NHE adventitious root tip elongation by affecting the elongation and maturation zones (Fig. 4d–e).

In general, Zn promoted the growth of the whole HE root system by increasing the number and length of lateral roots, which was further attributed to the rapid elongation of the root tip; however, no lateral root-promoting effects were observed in NHE under Zn treatment.

Zn concentration and accumulation

Both ecotypes showed significant differences in Zn concentrations and accumulation among the different Zn levels. At an external Zn supply of 100 or 250 μM, the Zn concentration in HE increased by 72.6% or 104.0% in roots, 7.0% or 29.4% in stems, and 48.4% or 59.2% in leaves, respectively, compared with the control (Fig. 1e–f). In contrast, low-Zn treatment decreased the Zn concentration in HE roots, stems, and leaves by 67.0%, 19.7%, and 37.8%, respectively. The variation trend of Zn accumulation was consistent with that of the Zn concentration. However, low-Zn treatment reduced the accumulation of Zn in HE roots, stems, and leaves by 69.1%, 37.7%, and 46.1%, respectively (Fig. 1g–h).

The spatial distribution of different elements was analyzed using nano-XRF in the lateral root and root tips of HE plants after different Zn exposures. The pixel brightness represents the elemental fluorescence intensity. As shown in Fig. 5, Zn (red) was scattered throughout the roots, Fe (green) accumulated in the epidermis, and K (blue) was mainly distributed in the cell wall. In HE roots at 250 μM Zn level, high fluorescence intensities of Zn were observed in the cortical intercellular space compared with the control (Fig. 5a–c). In NHE, higher Zn levels only increased the Zn signal intensity scattered in the root cells (Fig. 5b–d). In HE, the macroelements K, P, and S were mainly distributed in the root tip and base of the new lateral roots, and the trace element Fe was located in the epidermis of the primary root (Fig. 6b). In addition to the central pillar of the primary root, Zn accumulated in the elongation zone and in some “special parts” of the base of the lateral roots. To further explore the cell structure of these “special parts,” we selected elements with widely different distributions of Fe and K to co-localize with Zn in the lateral roots (Fig. 6). Based on the nano-XRF imaging and photomicrographs, Zn may specifically accumulate in the pericycle and extracellular regions of damaged primary roots.

Effects of Zn on root hormones

At the 100 μM Zn level, the content of auxin in HE roots was increased by 59.1%, 89.6%, 105.8%, and 125.5% at 1, 3, 6, and 12 h, respectively, compared with the control. After 24 h of exposure, the IAA content in HE roots reached a maximum of 66.5 ng/g (fresh weight), which was increased by 1.34 times compared to the control. After 3–7 days of treatment, it remained stable after a slight decrease (Fig. 7a). However, the IAA content in the NHE roots first increased and then decreased during the 7-day Zn treatment (Fig. 7b).

Auxin oxidase (indole acetic acid oxidase) is a type of enzyme that induces auxin degradation. The activity of IAA oxidase in HE roots was reduced by 17.4–54.2% under Zn exposure and reached a minimum 1.17 μmol/h/g after 7 days (Fig. 7c). However, IAA oxidase activity in NHE roots first increased and then decreased after Zn exposure. Compared with the control, IAA oxidase activity increased by

12.8% and 70.7% under 1 h and 7 d of Zn exposure, respectively. IAA oxidase activity increased by 2.94 times and reached a maximum 2.11 μmol/h/g under Zn exposure for 12 h.

Cytokinin content in the two ecotypes differed under Zn exposure. The cytokinin content in HE roots increased, whereas that in NHE roots decreased. After 6 h of Zn treatment, both ecotypes reached their maximum or minimum and then changed slightly (Fig. 7e,f).

Transcriptome analysis of roots

We used high-throughput sequencing technology to compare and analyze the changes and differences in the transcriptomes of HE roots under different Zn treatments. Among the 874 genes regulated by high Zn levels, 309 were upregulated and 565 were downregulated. To further study the specific metabolic pathways in HE under Zn stress, we carried out KEGG biological pathway analysis on the DEGs. The upregulated DEGs in roots were mainly involved in the processes of C5-branched dibasic acid and propionic acid metabolism in carbohydrate metabolism; nitrogen metabolism and carbon fixation in energy metabolism; and tryptophan biosynthesis, tyrosine biosynthesis, and metabolism in amino acid metabolism (Fig. 8). In contrast, the largest number of downregulated DEGs were mainly enriched in the ribosome (Fig. 9). The largest enrichment process was for the photosynthesis antenna protein, which was mainly involved in the processes of oxidative phosphorylation in energy metabolism, steroid and fatty acid biosynthesis, and linoleic acid metabolism in lipid metabolism.

Based on the transcriptome analysis, we further screened key gene resources (Fig. 10). The upregulated DEGs were associated with germin-like protein, auxin response factor, sugar transport protein, tryptophan metabolism, aminotransferase-related family protein, ammonium transporter, and urea active transporter. Downregulated DEGs were associated with wall-associated receptor kinase, serine/threonine protein kinase, polyamine oxidase, mitogen-activated protein kinase kinase, and serine/arginine-rich protein.

Discussion

High Zn enhanced plant growth and root development of S. alfredii

High concentrations of Zn can be harmful to plants. Zn toxicity inhibits root growth and affects nutrient absorption in plants (dos Santos et al. 2020). Our results showed that NHE were dwarfed with short roots under high Zn stress (Fig. 1a–b), which was consistent with the phenotype of plants after Zn poisoning. However, in HE roots under high-Zn treatment for 7 d, the total biomass, total root length, surface area, volume, number of lateral roots, and length of lateral roots increased. Our results indicated that high-Zn treatment promoted the growth of HE of *S. alfredii* roots and shoots.

Previous studies have also reported that high Zn levels can increase the biomass of HE shoots, especially by promoting the rapid growth of new shoots (Long et al. 2006). Li et al. reported that high Zn concentrations were beneficial for HE growth, and 500 μM Zn induced a significant increase in root biomass (Li et al. 2008). This is a very interesting phenomenon, indicating that HE not only has a high

tolerance to Zn but may also have high demands for Zn. It has been suggested that *S. alfredii* has evolved root foraging mechanisms associated with greater Zn requirements (Liu et al. 2010).

High Zn promotes HE growth through transport, compartmentalization, and regulation of auxin anabolism

Nano-XRF analysis showed that Zn was located in the cortical intercellular space of HE root cells to avoid excess Zn toxicity, whereas in NHE, Zn was scattered in the root cells (Fig. 5). The data indicate that more Zn was retained in NHE root cells, whereas HE transported Zn to the shoots. Previous studies have shown that HE root cells induce cell wall methylation and hemicellulose modification under Zn stress (Guo et al. 2020; Guo et al. 2020), which promotes root cell wall analysis and xylem transport of Zn to the shoots quickly and then participates in phloem remobilization transport (Lu et al. 2013). Previously, it has been observed that the epidermal layers serve as important storage sites for the accumulation of Zn in the HE of *S. alfredii* (Tian et al. 2009). These results are consistent with those of Dinh et al. who reported the Zn hyperaccumulator *Noccaea caerulescens* (Dinh et al. 2015). However, in NHE, a large amount of Zn is adsorbed on the cell wall or stored in vacuoles (Yang et al. 2006) and is not transported to the shoots. Plants can weaken the toxicity of heavy metals by accumulating heavy metals in their cell walls (Wang & Liu 2013).

Zn is an essential substance in the tryptophan-dependent auxin biosynthesis pathway (Wang et al. 2012), and auxin plays an important role in the development of lateral roots, affecting various stages of lateral root development (Motte et al. 2019). Our data showed that the auxin content of HE roots increased and the auxin oxidase activity decreased rapidly reducing the degradation of auxin under high-Zn treatment, while NHE roots exhibited the opposite effects. The effect of high Zn concentrations on cytokinin in HE and NHE roots was consistent with that of auxin (Fig. 7). Thus, the high Zn content in HE can effectively promote plant growth and root development by regulating the anabolism of auxin and cytokinin. A recent study found that excess Zn increases the expression of auxin biosynthesis-related genes and results in auxin accumulation in the root tips (Zhang et al. 2018). Studies have found that auxin may also affect the process of Zn absorption by plants. Zn deficiency can increase the expression of the Zn transport-related genes OsIRT1, OsZIP4, and OsZIP1 in rice roots; however, these genes were significantly downregulated after blocking the auxin signal, indicating that auxin is involved in the absorption and transport of Zn in rice when Zn is deficient (Begum et al. 2016).

In summary as to how Zn promotes the growth of HE plants, HE reduces the inhibitory effect of excessive Zn accumulation on root cells through efficient transport to the shoots and root cell apoplast compartments. In contrast, Zn accumulation in HE roots regulates the anabolism of growth hormones and effectively promotes lateral root germination and root growth.

HE of S. alfredii suffers adversity under low Zn conditions while it prospers under high Zn conditions

KEGG analysis of HE root cells revealed that the upregulated DEGs were mainly enriched in the regulation of carbohydrate metabolism, nitrogen metabolism and carbon fixation, and tryptophan biosynthesis. The predicted functions of the upregulated DEGs were related to germin-like proteins (GLPs), auxin response factor (ARF), tryptophan (Trp) metabolism, sugar transport proteins, ammonium (AMT) and urea transporters (UAT) (Fig. 10). Various germin-like proteins are known to be involved in the growth and development of root tissues (Dunwell et al. 2008). Overexpression of *Arabidopsis* Plasmodesmata germin-like proteins reduces primary root growth but enhances lateral root growth by regulating the phloem-mediated allocation of resources between the primary and lateral root meristems (Ham et al. 2012). Auxin biosynthesis via the tryptophan aminotransferase of arabidopsis (TAA)/YUCCA (YUC) route involving tryptophan aminotransferases and YUC flavin-dependent monooxygenases that produce the auxin indole-3-acetic acid (IAA) from tryptophan is currently the most researched auxin biosynthetic pathway (Poulet & Kriechbaumer 2017). Tryptophan aminotransferases (TAA1/TARs) catalyze the first step in the conversion of L-tryptophan to indole-3-pyruvic acid (Kakei et al. 2017). The auxin response factor (ARF) family functions by binding to auxin response elements (AuxREs) on the promoters of auxin response genes, activating or repressing them, leading to plant growth (Guilfoyle & Hagen 2007). Sugars are essential carbohydrates generated by photosynthesis in source leaves and are then transferred through the phloem to sink organs such as seeds, fruits, stems, tubers, and swollen taproots (Wen et al. 2022). Sugar-transport proteins play a crucial role in the cell-to-cell and long-distance distribution of sugars in plants (Williams et al. 2000). Ammonium transporters can transport ammonium from the roots to the shoots to mediate the acquisition of ammonium nitrogen from the soil, which is essential to meet the nitrogen demand of plants (Hao et al. 2020).

The downregulated DEGs were mainly involved in the regulation of oxidative phosphorylation in energy metabolism, steroid and fatty acid biosynthesis in lipid metabolism, and linoleic acid metabolism. These metabolic processes are associated with plant stress responses. Under Zn-deficient conditions, resistant plants can reduce this damage via lipid remodeling (Ruelland et al. 2015). Fatty acids play an important role in plant plasma membrane stability, stress resistance, tissue senescence (Rontani et al. 2005), and seed development (Smith et al. 2003). The predicted functions of the downregulated DEGs were also related to plant stress responses. The wall-associated kinase (WAK) gene family, a receptor-like kinase gene family in plants, plays important roles in cell expansion, pathogen resistance, and heavy-metal stress tolerance in *Arabidopsis thaliana* (Zhang et al. 2005). Polyamines not only play roles in plant growth and development but also in adaptation to environmental stresses. Previous studies have shown that maize polyamine oxidase (PAO) plays a role in cell wall maturation and root differentiation by producing H_2O_2 (Cona et al. 2005; Rea et al. 2004). Gomez-Jimenez et al. reported that PAO and DAO have significant functions in olive fruit abscission zone (AZ) development by providing apoplastic H_2O_2 for cell wall strengthening and lignosuberization events, and that a peroxidase substrate is provided in these cells throughout AZ development (Gomez-Jimenez et al. 2010). Plant MAPK cascades regulate numerous processes, including various environmental stress responses, hormones, cell division, and developmental processes. Jasmonic acid (JA) and its methyl ester (MeJA) are plant signaling compounds involved in regulating stress responses and development. Several studies have revealed that

some MAPK cascades are involved in the wound/JA signaling pathway (Kumar et al. 2013). Serine/arginine-rich (SR) proteins are conserved RNA-binding proteins that play a major role in RNA metabolism. Stress signals control both the phosphorylation status and subcellular localization of plant SR proteins, indicating potential mechanistic links between abiotic stress and the regulation of alternative splicing (Duque 2011).

This indicates that there are two reasons for the growth-promoting effects of high Zn levels on HE. Upregulated key genes, such as auxin synthesis, carbohydrate synthesis and metabolism, and amino acid metabolism, provide an energy basis for the growth and development of roots. In contrast, the downregulated genes were related to Zn deficiency stress, implying that high Zn levels alleviated this stress in HE roots. This indicates that HE suffers adversity under low-Zn conditions and exhibits a stress response, whereas high Zn provides conditions for HE to prosper (Fig. 11).

In conclusion, this study highlights the positive effect of high Zn concentrations on the growth of the Zn/Cd hyperaccumulator *Sedum alfredii* Hance. At a 250 μM Zn level, HE root biomass and Zn concentration in roots increased while those in NHE were reduced. Nano-XRF analysis showed that Zn was located in the cortical intercellular space in HE roots, whereas Zn was scattered in the root cells of NHE. The auxin content in HE roots was increased and the auxin oxidase activity decreased after exposure to 100 μM Zn, while NHE exhibited the opposite effects. To adapt to high Zn conditions, HE cells upregulated genes related to carbohydrate metabolism, nitrogen metabolism, carbon fixation, and tryptophan biosynthesis, and downregulated genes related to lipid metabolism and linoleic acid metabolism. We further screened key gene resources, laying a foundation for the molecular mechanism underlying the positive effect of high Zn conditions on HE growth. This study provides a theoretical reference for the optimization of phytoremediation technologies for heavy metal-contaminated soil.

Declarations

Funding: This work was supported by projects from the National Natural Science Foundation of China (Nos. 41977130 and 41877116) and the Natural Science Foundation of Zhejiang Province (No. LZ22D010004).

Competing Interests: The authors have no relevant financial or non-financial interests to disclose.

Author Contributions: All authors contributed to the conception and design of this study. Material preparation, data collection, and analysis were performed by Yuxiao Gao and Haiyue Yu. The first draft of the manuscript was written by Yuxiao Gao and Lingli Lu, reviewed and revised by Haizhong Lin. All authors commented on previous versions of the manuscript. All authors read and approved the final version of the manuscript.

Data Availability: The datasets generated during and analysed during the current study are available from the corresponding author on reasonable request.

References

1. Anjum NA, Singh HP, Khan MIR et al. (2015) Too much is bad-an appraisal of phytotoxicity of elevated plant-beneficial heavy metal ions. Environmental Science and Pollution Research 22(5): 3361-3382. https://doi.org/10.1007/s11356-014-3849-9
2. Azhar H, Ahmad Z, Allah D et al. (2020) Production and implication of bio-activated organic fertilizer enriched with zinc-solubilizing bacteria to boost up maize (Zea mays L.) production and biofortification under two cropping seasons. Agronomy 10(1): 39-56. https://doi.org/10.3390/agronomy10010039
3. Begum MC, Islam M, Sarkar MR et al. (2016) Auxin signaling is closely associated with Zn-efficiency in rice (Oryza sativa L.). Journal of Plant Interactions 11(1): 124-129. https://doi.org/10.1080/17429145.2016.1220026
4. Broadley MR, White PJ, Hammond JP et al. (2007) Zinc in plants. New Phytologist 173(4): 677-702. https://doi.org/10.1111/j.1469-8137.2007.01996.x
5. Cona A, Moreno S, Cenci F et al. (2005) Cellular re-distribution of flavin-containing polyamine oxidase in differentiating root and mesocotyl of Zea mays L. seedlings. Planta 221(2): 265-276. https://doi.org/10.1007/s00425-004-1435-y
6. Ding H, Zhu W, Yang S, Yang X. (2005) Dynamic changes in antioxidative systems in roots of tomato (Lycopersicom esculentum Mill.) seedling under zinc stress and recovery. Chinese Journal of Applied and Environmental Biology 11(5): 531-535.
7. Dinh NT, Vu DT, Mulligan D, Nguyen AV. (2015) Accumulation and distribution of zinc in the leaves and roots of the hyperaccumulator Noccaea caerulescens. Environmental and Experimental Botany 110: 85-95. https://doi.org/10.1016/j.envexpbot.2014.10.001
8. dos Santos LR, da Silva BRS, Pedron T et al. (2020) 24-Epibrassinolide Improves Root Anatomy and Antioxidant Enzymes in Soybean Plants Subjected to Zinc Stress. Journal of Soil Science and Plant Nutrition 20(1): 105-124. https://doi.org/10.1007/s42729-019-00105-z
9. Dunwell JM, Gibbings JG, Mahmood T, Naqvi SMS. (2008) Germin and germin-like proteins: Evolution, structure, and function. Critical Reviews in Plant Sciences 27(5): 342-375. https://doi.org/10.1080/07352680802333938
10. Duque P. (2011) A role for SR proteins in plant stress responses. Plant Signaling & Behavior 6(1): 49-54. https://doi.org/10.4161/psb.6.1.14063
11. Edelstein M, Ben-Hur M. (2018) Heavy metals and metalloids: Sources, risks and strategies to reduce their accumulation in horticultural crops. Scientia Horticulturae 234: 431-444. https://doi.org/10.1016/j.scienta.2017.12.039
12. Glinska S, Gapinska M, Michlewska S et al. (2016) Analysis of Triticum aestivum seedling response to the excess of zinc. Protoplasma 253(2): 367-377. https://doi.org/10.1007/s00709-015-0816-3
13. Gomez-Jimenez MC, Paredes MA, Gallardo M, Sanchez-Calle IM. (2010) Mature fruit abscission is associated with up-regulation of polyamine metabolism in the olive abscission zone. Journal of

Plant Physiology 167(17): 1432-1441. https://doi.org/10.1016/j.jplph.2010.05.020

14. Gong H-m, Shen Y. (2010) Research Progress in Mechanisms of Plant Tolerance to Zinc. Acta Botanica Boreali-Occidentalia Sinica 30(3): 633-644.
15. Guilfoyle TJ, Hagen G. (2007) Auxin response factors. Current Opinion in Plant Biology 10(5): 453-460. https://doi.org/10.1016/j.pbi.2007.08.014
16. Guo X, Liu Y, Zhang R et al. (2020) Hemicellulose modification promotes cadmium hyperaccumulation by decreasing its retention on roots in Sedum alfredii. Plant and Soil 447(1-2): 241-255. https://doi.org/10.1007/s11104-019-04339-9
17. Guo X, Luo J, Du Y et al. (2020) Coordination between root cell wall thickening and pectin modification is involved in cadmium accumulation in Sedum alfredii. Environmental Pollution 268(Pt A): 115665. https://doi.org/10.1016/j.envpol.2020.115665
18. Guo X, Yan C, Ye B. (2009) Effect of Cd-Zn Combined Stress on Contents of Osmotic Substances in Kandelia candel (L.) Druce Seedlings. Chinese Journal of Applied and Environmental Biology 15(3): 308-312. https://doi.org/10.3724/sp.J.1145.2009.00308
19. Ham BK, Li G, Kang BH et al. (2012) Overexpression of Arabidopsis Plasmodesmata Germin-Like Proteins Disrupts Root Growth and Development. Plant Cell 24(9): 3630-3648. https://doi.org/10.1105/tpc.112.101063
20. Hao DL, Zhou JY, Yang SY et al. (2020) Function and Regulation of Ammonium Transporters in Plants. International Journal of Molecular Sciences 21(10): 3557. https://doi.org/10.3390/ijms21103557
21. Kakei Y, Nakamura A, Yamamoto M et al. (2017) Biochemical and Chemical Biology Study of Rice OsTAR1 Revealed that Tryptophan Aminotransferase is Involved in Auxin Biosynthesis: Identification of a Potent OsTAR1 Inhibitor, Pyruvamine2031. Plant and Cell Physiology 58(3): 598-606. https://doi.org/10.1093/pcp/pcx007
22. Kumar K, Wankhede Dhammaprakash P, Sinha Alok K. (2013) Signal convergence through the lenses of MAP kinases: paradigms of stress and hormone signaling in plants. Frontiers in Biology 8(1): 109-118.
23. Li T, Yang X, Lu L et al. (2009) Effects of zinc and cadmium interactions on root morphology and metal translocation in a hyperaccumulating species under hydroponic conditions. Journal of Hazardous Materials 169(1-3): 734-741. https://doi.org/10.1016/j.jhazmat.2009.04.004
24. Li TQ, Lu LL, Zhu E et al. (2008) Antioxidant Responses in Roots of Two Contrasting Sedum alfredii Hance Ecotypes under Elevated Zinc Concentrations. Russian Journal of Plant Physiology 55(6): 799-807. https://doi.org/10.1134/s1021443708060095
25. Li TQ, Yang XE, Jin XF et al. (2005) Root responses and metal accumulation in two contrasting ecotypes of Sedum alfredii Hance under lead and zinc toxic stress. Journal of Environmental Science and Health Part A 40(5): 1081-1096. https://doi.org/10.1081/ese-200056163
26. Liu FJ, Tang YT, Du RJ et al. (2010) Root foraging for zinc and cadmium requirement in the Zn/Cd hyperaccumulator plant Sedum alfredii. Plant and Soil 327(1-2): 365-375.

https://doi.org/10.1007/s11104-009-0060-8

27. Liu Y, Donner E, Lombi E et al. (2013) Assessing the contributions of lateral roots to element uptake in rice using an auxin-related lateral root mutant. Plant and Soil 372(1-2): 125-136. https://doi.org/10.1007/s11104-012-1582-z
28. Long X, Ni W, Ye Z, Yang X. (2006) Zinc tolerance and hyperaccumulation of Sedum alfredii Hance: A greenhouse experiment with artificial polluted soils. Bulletin of Environmental Contamination and Toxicology 76(2): 264-270. https://doi.org/10.1007/s00128-006-0916-z
29. Lu L-l, Tian S-k, Yang X-e et al. (2008) Enhanced root-to-shoot translocation of cadmium in the hyperaccumulating ecotype of Sedum alfredii. Journal of Experimental Botany 59(11): 3203-3213. https://doi.org/10.1093/jxb/ern174
30. Lu L, Tian S, Zhang J et al. (2013) Efficient xylem transport and phloem remobilization of Zn in the hyperaccumulator plant species Sedum alfredii. New Phytologist 198(3): 721-731. https://doi.org/10.1111/nph.12168
31. Mehta SK, Gaur JP. (1999) Heavy-metal-induced proline accumulation and its role in ameliorating metal toxicity in Chlorella vulgaris. New Phytologist 143(2): 253-259. https://doi.org/10.1046/j.1469-8137.1999.00447.x
32. Motte H, Vanneste S, Beeckman T. (2019) Molecular and environmental regulation of root development. Annual Review of Plant Biology 70: 465-488. https://doi.org/10.1146/annurev-arplant-050718-100423
33. Neumann D, zur Nieden U. (2001) Silicon and heavy metal tolerance of higher plants. Phytochemistry 56(7): 685-692. https://doi.org/10.1016/s0031-9422(00)00472-6
34. Noreen S, Sultan M, Akhter MS et al. (2021) Foliar fertigation of ascorbic acid and zinc improves growth, antioxidant enzyme activity and harvest index in barley (Hordeum vulgare L.) grown under salt stress. Plant Physiology and Biochemistry 158: 244-254. https://doi.org/10.1016/j.plaphy.2020.11.007
35. Pavia I, Roque J, Rocha L et al. (2019) Zinc priming and foliar application enhances photoprotection mechanisms in drought-stressed wheat plants during anthesis. Plant Physiology and Biochemistry 140: 27-42. https://doi.org/10.1016/j.plaphy.2019.04.028
36. Poulet A, Kriechbaumer V. (2017) Bioinformatics Analysis of Phylogeny and Transcription of TAA/YUC Auxin Biosynthetic Genes. International Journal of Molecular Sciences 18(8): 1791. https://doi.org/10.3390/ijms18081791
37. Rea G, de Pinto MC, Tavazza R et al. (2004) Ectopic expression of maize polyamine oxidase and pea copper amine oxidase in the cell wall of tobacco plants. Plant Physiology 134(4): 1414-1426. https://doi.org/10.1104/pp.103.036764
38. Rontani JF, Rabourdin A, Pinot F et al. (2005) Visible light-induced oxidation of unsaturated components of cutins: a significant process during the senescence of higher plants. Phytochemistry 66(3): 313-321. https://doi.org/10.1016/j.phytochem.2004.12.015

39. Ruelland E, Kravets V, Derevyanchuk M et al. (2015) Role of phospholipid signalling in plant environmental responses. Environmental and Experimental Botany 114: 129-143. https://doi.org/10.1016/j.envexpbot.2014.08.009
40. Smith MA, Moon H, Chowrira G, Kunst L. (2003) Heterologous expression of a fatty acid hydroxylase gene in developing seeds of Arabidopsis thaliana. Planta 217(3): 507-516. https://doi.org/10.1007/s00425-003-1015-6
41. Sun Y, Luo W, Li X, Chen B. (2008) The effect of Zn~(2+)on physiological characteristics of cucumber during seed germination. Ecology and Environment 17(1): 307-311.
42. Tavallali V. (2017) Interactive effects of zinc and boron on growth, photosynthesis, and water relations in pistachio. Journal of Plant Nutrition 40(11): 1588-1603. https://doi.org/10.1080/01904167.2016.1270308
43. Tian S-K, Lu L-L, Yang X-E et al. (2009) Stem and leaf sequestration of zinc at the cellular level in the hyperaccumulator Sedum alfredii. New Phytologist 182(1): 116-126. https://doi.org/10.1111/j.1469-8137.2008.02740.x
44. Tian S, Lu L, Zhang J et al. (2011) Calcium protects roots of Sedum alfredii H. against cadmium-induced oxidative stress. Chemosphere 84(1): 63-69. https://doi.org/10.1016/j.chemosphere.2011.02.054
45. Wang C, Zhang SH, Wang PF et al. (2009) The effect of excess Zn on mineral nutrition and antioxidative response in rapeseed seedlings. Chemosphere 75(11): 1468-1476. https://doi.org/10.1016/j.chemosphere.2009.02.033
46. Wang J, Liu D, Guo X, Zhang A. (2012) Research Advances in Auxin Biosynthesis. Chinese Bulletin of Botany 47(3): 292-301.
47. Wang JH, Moeen-ud-din M, Yang SH. (2021) Dose-dependent responses of Arabidopsis thaliana to zinc are mediated by auxin homeostasis and transport. Environmental and Experimental Botany 189: 104554. https://doi.org/10.1016/j.envexpbot.2021.104554
48. Wang XW, Liu ZF. (2013) The Subcellular Distributions of Cadmium, Chromium, Copper, Plumbum and Zinc in Hyperaccumulator and Accumulator. 2nd International Conference on Energy and Environmental Protection (ICEEP 2013) 726-731: 2434-2437.
49. Wen S, Neuhaus HE, Cheng J, Bie Z. (2022) Contributions of sugar transporters to crop yield and fruit quality. Journal of Experimental Botany 73(8): 2275-2289. https://doi.org/10.1093/jxb/erac043
50. Williams LE, Lemoine R, Sauer N. (2000) Sugar transporters in higher plants - A diversity of roles and complex regulation. Trends in Plant Science 5(7): 283-290. https://doi.org/10.1016/s1360-1385(00)01681-2
51. Xie RH, Zhao JQ, Lu LL et al. (2020) Seasonal Zinc Storage and a Strategy for Its Use in Buds of Fruit Trees. Plant Physiology 183(3): 1200-1212. https://doi.org/10.1104/pp.19.01563
52. Xu Q-S, Shi G-X, Wang X, Wu G-R. (2006) Generation of active oxygen and change of antioxidant enzyme activity in Hydrilla verticillata under Cd, Cu and Zn stress. Acta Hydrobiologica Sinica 30(1): 107-112.

53. Yang X, Li T, Yang J et al. (2006) Zinc compartmentation in root, transport into xylem, and absorption into leaf cells in the hyperaccumulating species of Sedum alfredii Hance. Planta 224(1): 185-195. https://doi.org/10.1007/s00425-005-0194-8
54. Yang XE, Long XX, Ye HB et al. (2004) Cadmium tolerance and hyperaccumulation in a new Zn-hyperaccumulating plant species (Sedum alfredii Hance). Plant and Soil 259(1-2): 181-189. https://doi.org/10.1023/B:PLSO.0000020956.24027.f2
55. Ye HB, Yang XE, He B et al. (2003) Growth response and metal accumulation of Sedum alfredii to Cd/Zn complex-polluted ion levels. Acta Botanica Sinica 45(9): 1030-1036.
56. Zhang P, Sun L, Qin J et al. (2018) cGMP is involved in Zn tolerance through the modulation of auxin redistribution in root tips. Environmental and Experimental Botany 147: 22-30. https://doi.org/10.1016/j.envexpbot.2017.10.025
57. Zhang SB, Chen C, Li L et al. (2005) Evolutionary expansion, gene structure, and expression of the rice wall-associated kinase gene family. Plant Physiology 139(3): 1107-1124. https://doi.org/10.1104/pp.105.069005

Figures

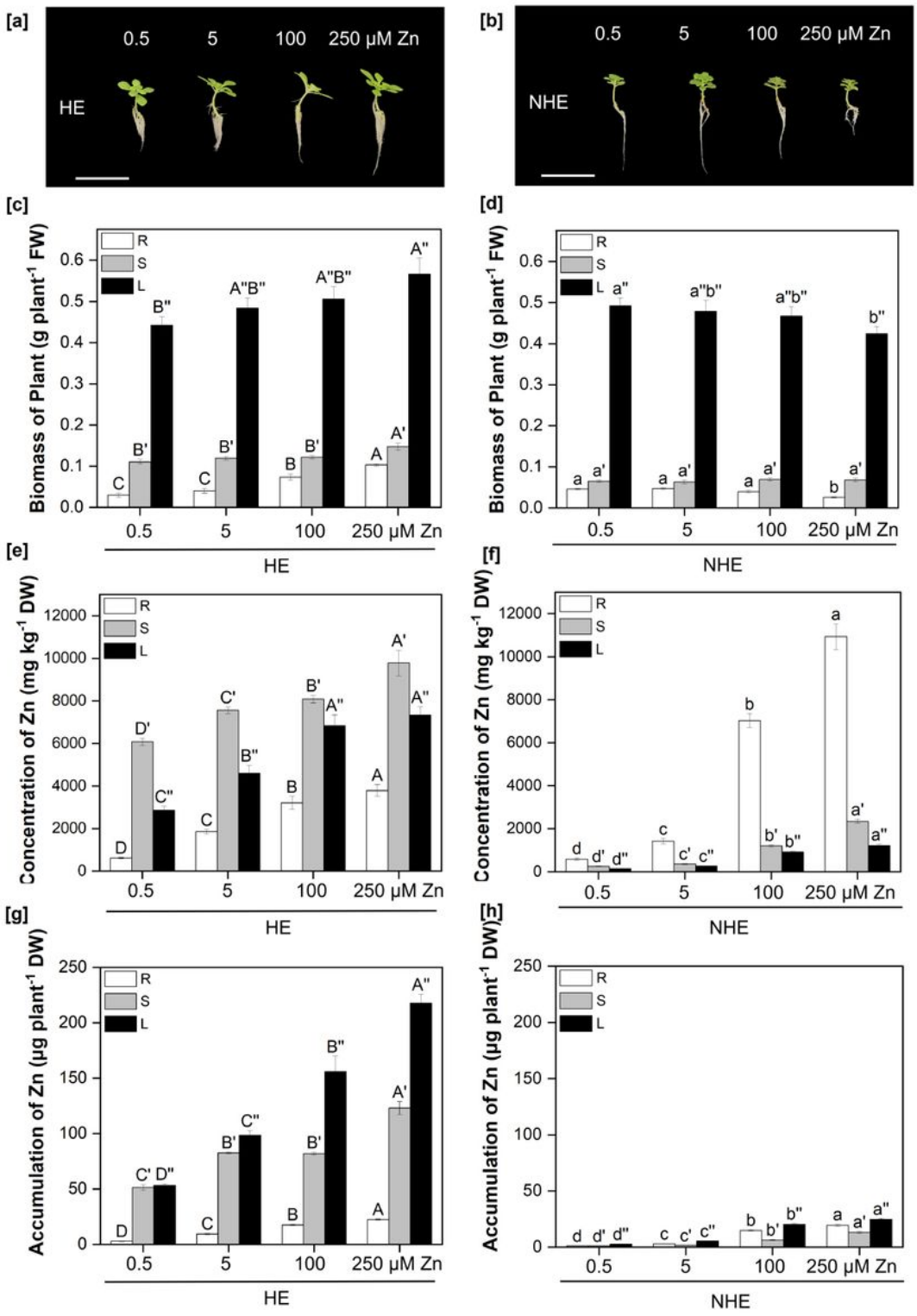


Figure 1

Hyperaccumulating ecotype (HE) and non-hyperaccumulating ecotype (NHE) of *Sedum alfredii* Hance treated with 0.5, 5, 100, or 250 μM Zn for 7 days. (a) Side view of HE. Scale bar: 10 cm (b) Side view of NHE. Scale bar: 10 cm (c) Biomass of HE (d) Biomass of NHE (e) Concentration of Zn in HE (f) Concentration of Zn in NHE (g) Accumulation of Zn in HE (h) Accumulation of Zn in NHE. Bars represent means ± SD (n=5), and different letters denote significant ($P<0.05$) differences within treatments.

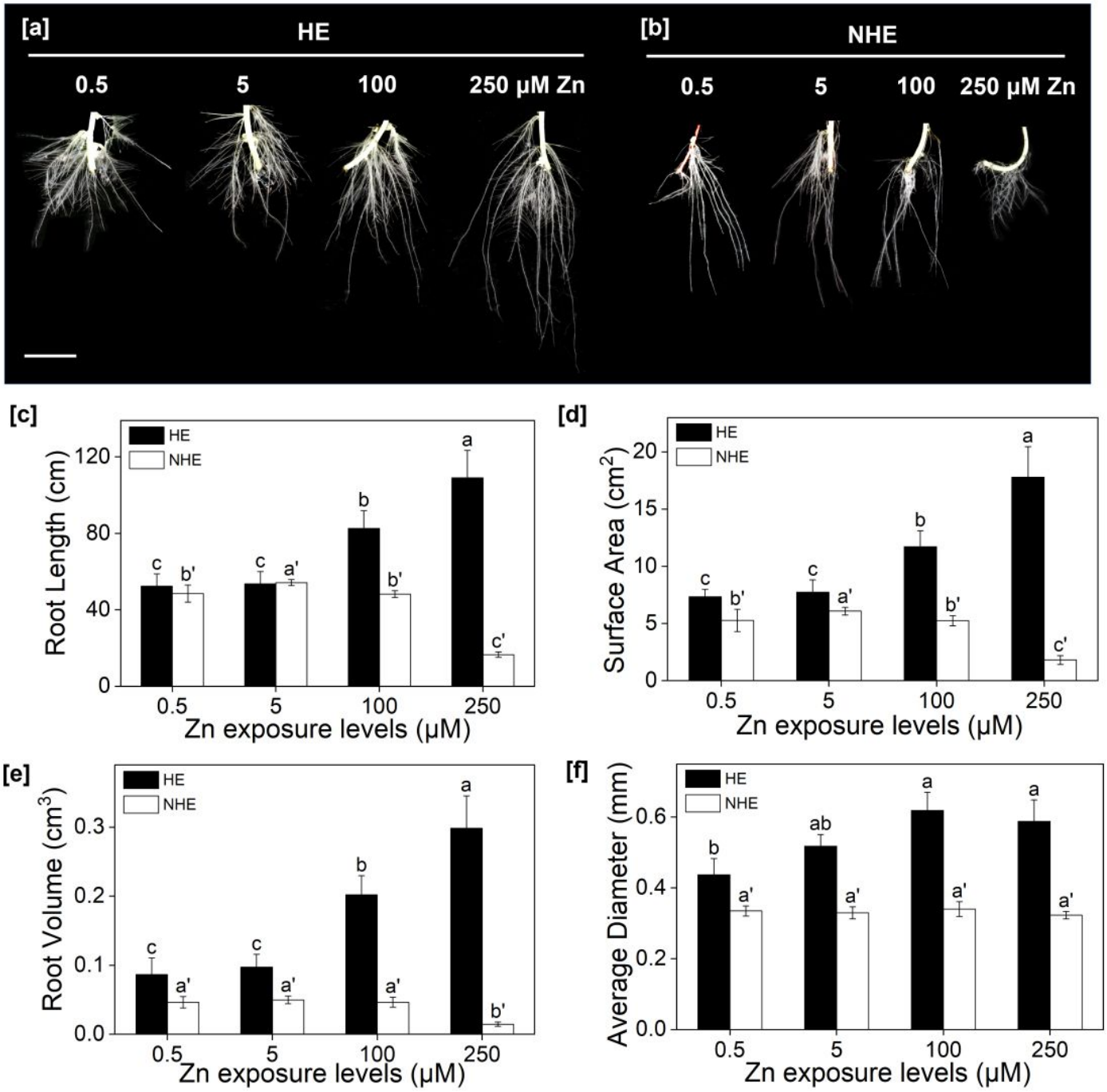


Figure 2

Roots of (a) hyperaccumulating ecotype (HE) and (b) non-hyperaccumulating ecotype (NHE) of *Sedum alfredii* Hance treated with 0.5, 5, 100, or 250 μM Zn for 7 days. Scale bar: 2 cm. (c) Root length, (d) root surface area, (e) root volume, and (f) average diameter of HE and NHE *Sedum alfredii* Hance treated with 0.5, 5, 100, or 250 μM Zn for 7 days. Bars represent means ± SD (n=7), and different letters denote significant ($P<0.05$) differences within treatments.

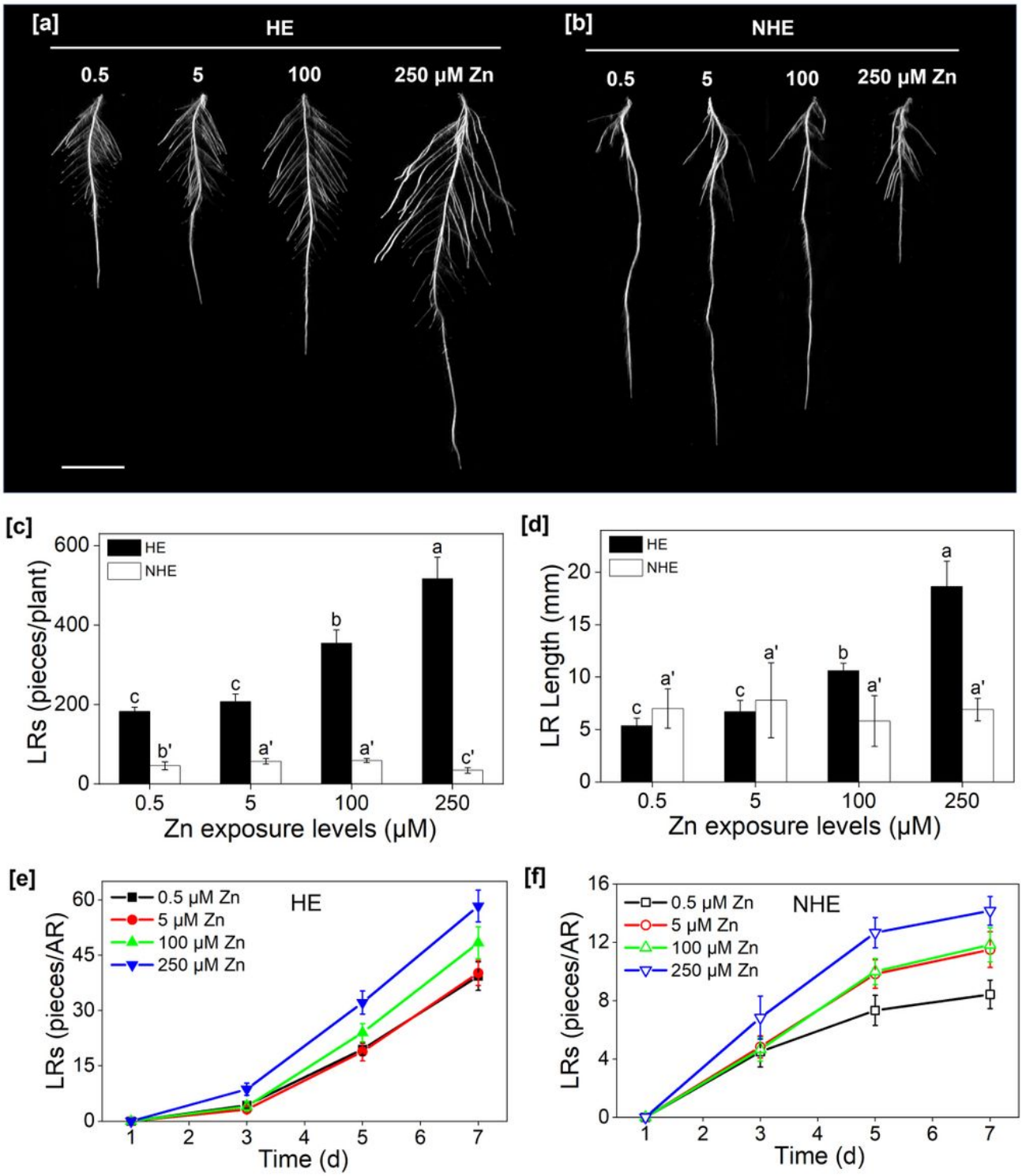


Figure 3

Differences in lateral roots of hyperaccumulating ecotype (HE) and non-hyperaccumulating ecotype (NHE) of *Sedum alfredii* Hance treated with 0.5, 5, 100, or 250 μM Zn for 7 days. Lateral roots of (a) HE and (b) NHE. Scale bar: 1 cm. (c) Lateral root numbers of each plant. (d) Average lateral root length. Average lateral root numbers of each adventitious root of (e) HE and (f) NHE. Bars represent means ± SD

(n=7), and different letters denote significant (P<0.05) differences within treatments. LR, lateral root; AR, adventitious root.

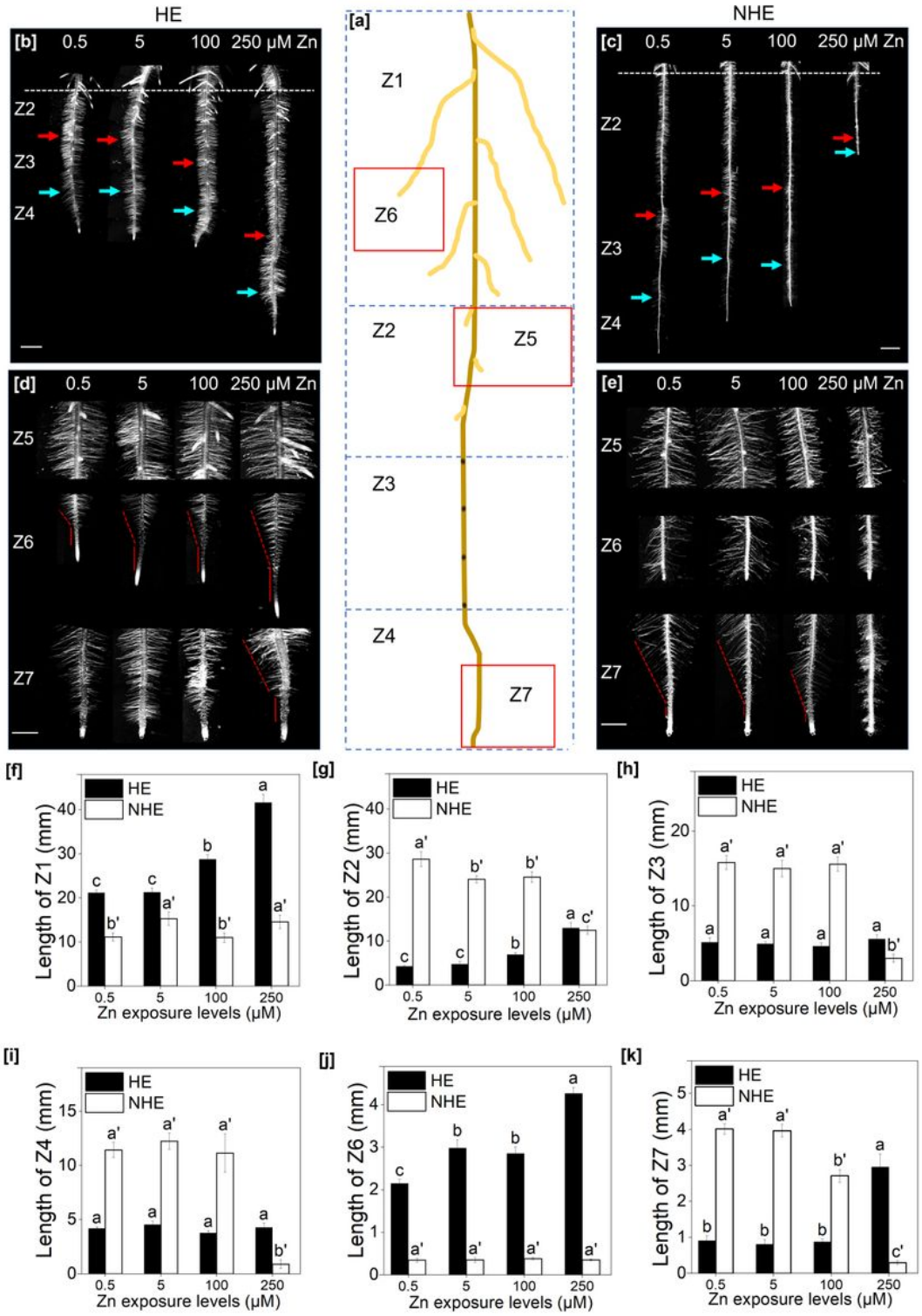


Figure 4

Differences in root zone of hyperaccumulating ecotype (HE) and non-hyperaccumulating ecotype (NHE) of *Sedum alfredii* Hance treated with 0.5, 5, 100, or 250 μM Zn for 7 days. (a) Different root zones. (b) Z2,

Z3, and Z4 of HE. Scale bar: 2 mm. (c) Z2, Z3, and Z4 of NHE. Scale bar: 4 mm. (d) Z5, Z6, and Z7 of HE. Scale bar: 1 mm. (e) Z5, Z6, and Z7 of NHE. Scale bar: 1 mm. Length of (f) Z1, (g) Z2, (h) Z3, (i) Z4, (j) Z6, and (k) Z7 of HE and NHE. Bars represent means ± SD (n=5), and different letters denote significant ($P<0.05$) differences within treatments. Z1, Mature lateral root zone; Z2, New lateral root zone; Z3, Lateral root primordium zone; Z4, No lateral root zone; Z5, New germination lateral root zone; Z6, Lateral root apex; Z7, Adventitious root apex. Brown line, Adventitious root; Yellow line, Lateral root; Black dot, Lateral root primordium; White dotted line, Boundary between Z1 and Z2; Red arrow, Boundary between Z2 and Z3; Blue arrow, Boundary between Z3 and Z4; Red dotted line, Mature zone of root apex; Red line, Elongation zone of root apex.

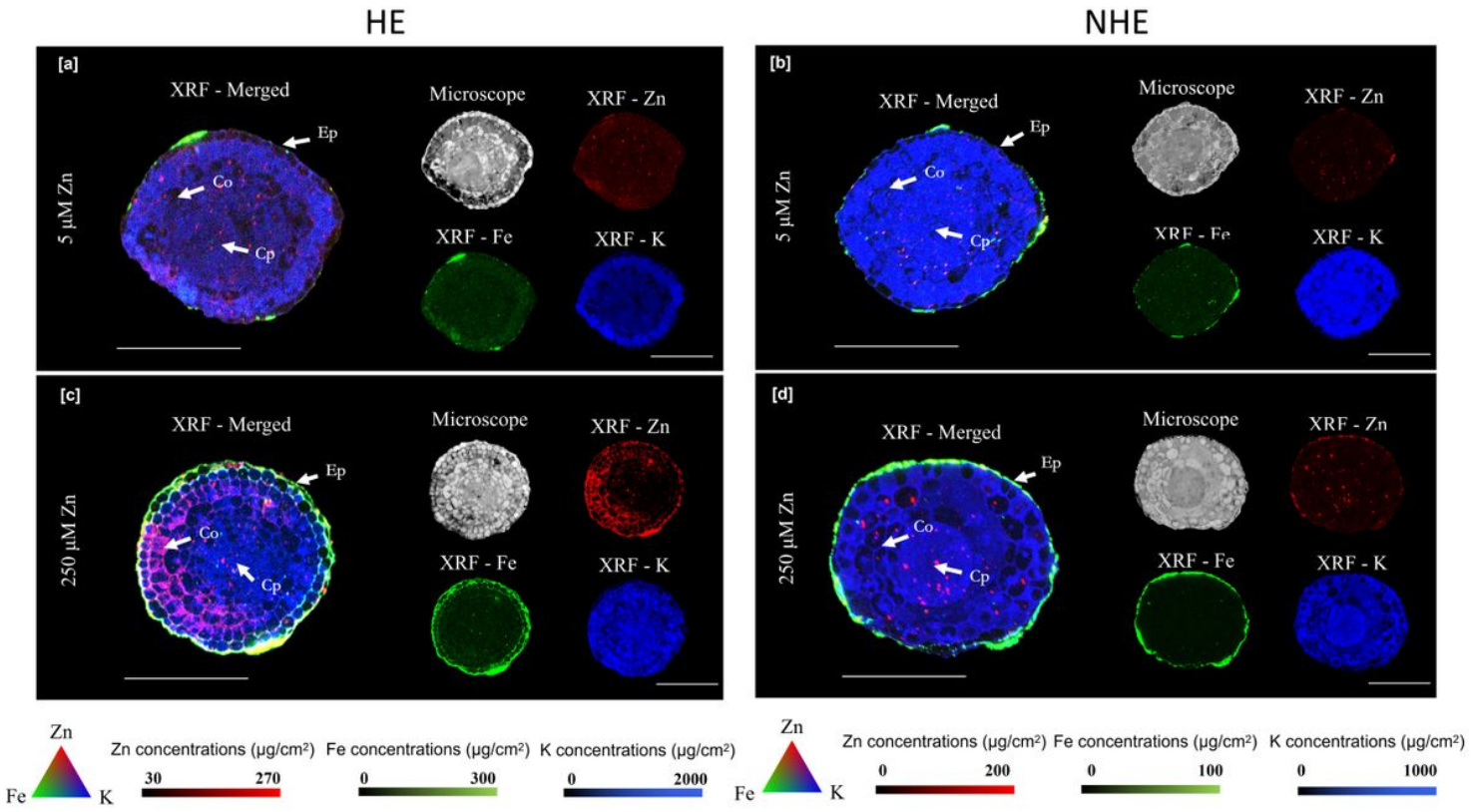


Figure 5

In vivo imaging of Zn, Fe, and K by micro X-ray in different root tips collected from plants of the hyperaccumulating ecotype (HE) of *Sedum alfredii*Hance treated with (a) 5 or (b) 250 µM Zn for 7 days and non-hyperaccumulating ecotype (NHE) treated with (c) 5 or (d) 250 µM Zn for 7 days. The red, green, and blue colors respectively depict the elemental concentration of Zn, Fe, and K in the map, scaled to the maximum value for each map. Scale bar: 100 µm. Ep, Epidermis; Co, Cortex; Cp, Center pillar.

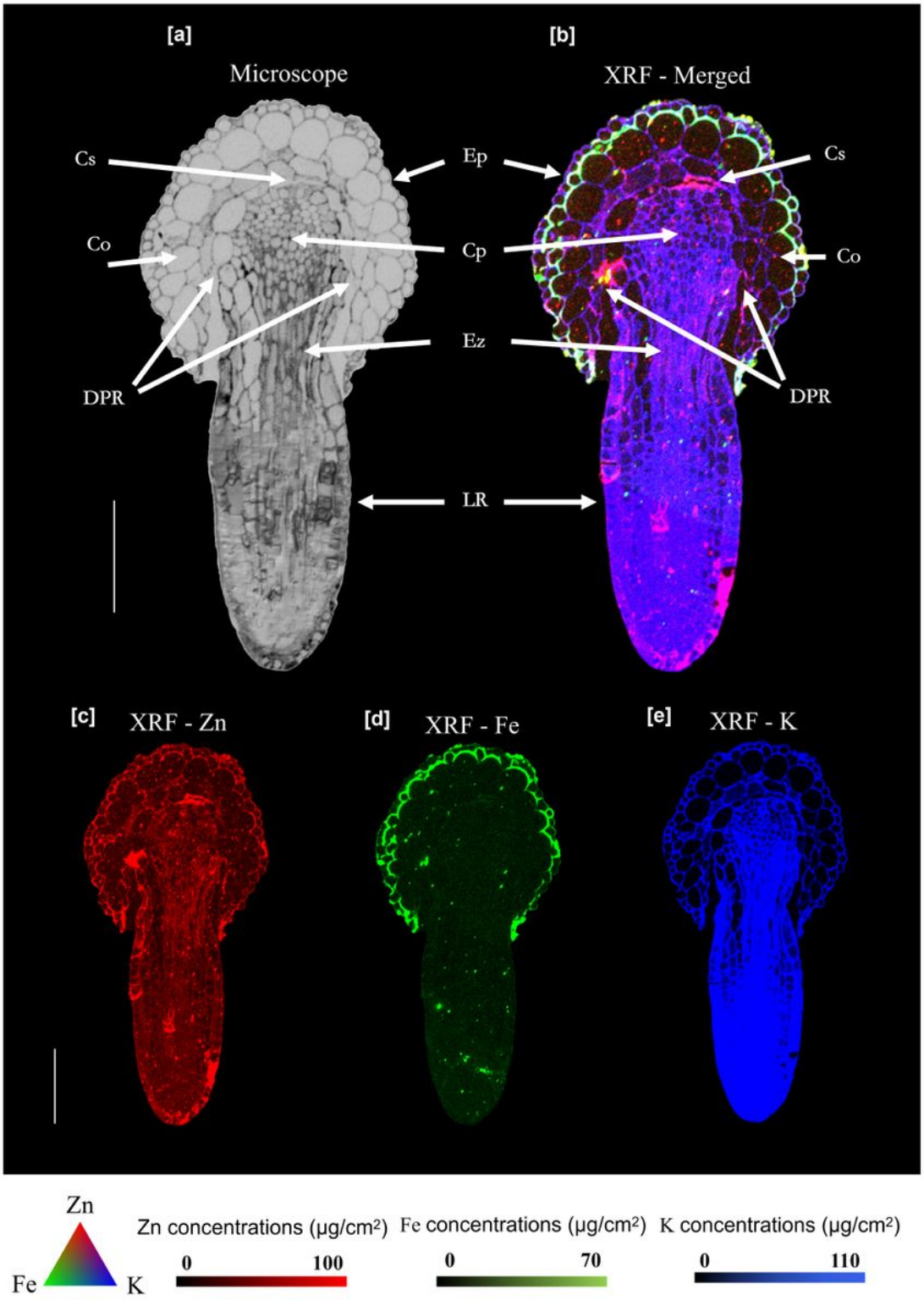


Figure 6

In vivo imaging using (a) microscope and (b) merged (c) Zn, (d) Fe, and (e) K by micro X-ray in different lateral roots collected from plants of the hyperaccumulating ecotype of *Sedum alfredii* Hance treated with 250 µM Zn for 7 days. The red, green, and blue colors respectively depict the elemental concentration of Zn, Fe, and K in the map scaled to the maximum value for each map. Scale bar: 100 µm. Ep, Epidermis;

Co, Cortex; Cp, Center pillar; Cs, Central sheath; Ez, Elongation zone; DPR, Damaged primary root; LR, Lateral root.

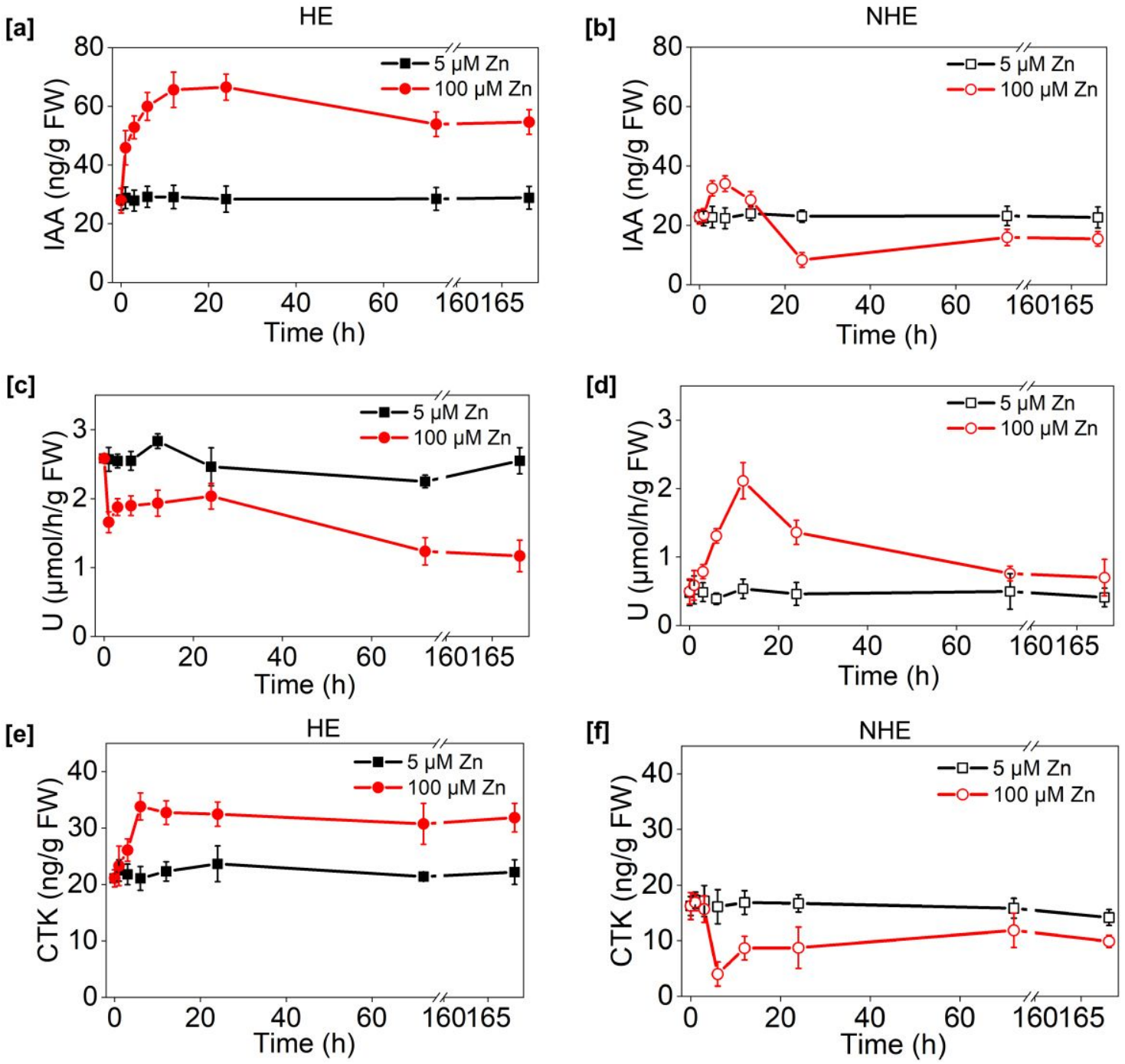


Figure 7

Differences in the auxin (IAA) concentration, IAA oxidase activity, and cytokinin (CTK) concentration in roots of hyperaccumulating ecotype (HE) and non-hyperaccumulating ecotype (NHE) of *Sedum alfredii* Hance treated with 5 or 100 μM Zn for 0, 1, 3, 6, 12, or 24 hours or 3 or 7 days. (a) Concentration of IAA in HE roots. (b) Concentration of IAA in NHE roots. (c) IAA oxidase activity in HE roots. (d) IAA oxidase activity in NHE roots. (e) Concentration of CTK in HE roots. (f) Concentration of CTK in NHE roots. Bars represent means ± SD (n=3). IAA, Indole acetic acid.

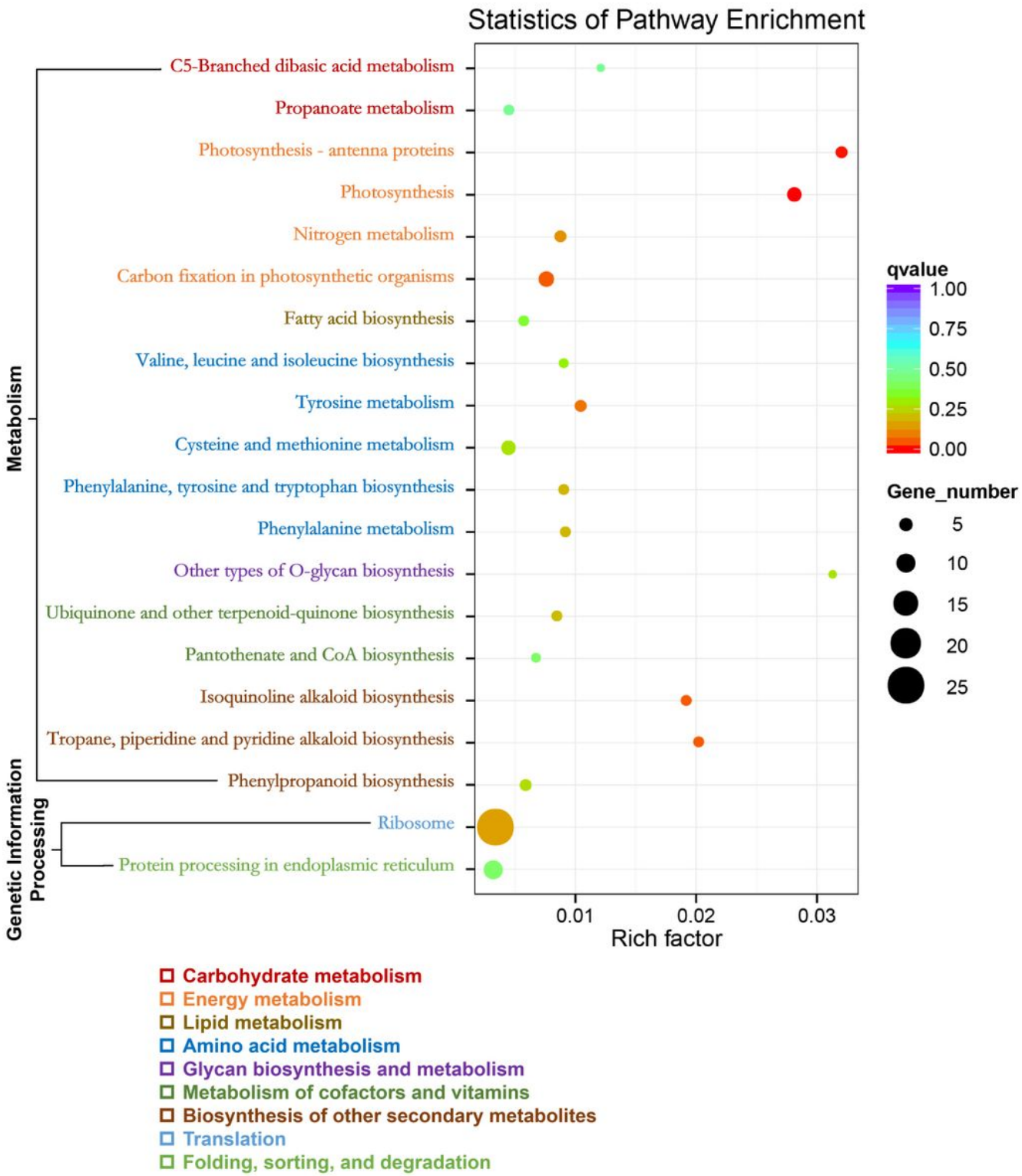


Figure 8

KEGG analysis of differentially expressed upregulated genes in root cells of hyperaccumulating ecotype of *S. alfredii* treated with 5 or 100 μM Zn for 24 h. The abscissa indicates the enrichment factor; the size indicates the number of genes; the color indicates the significance, the redder the color indicates the more significant the degree of enrichment; the ordinate indicates the metabolic pathway with the higher degree of enrichment; and the annotation color is classified according to the pathway.

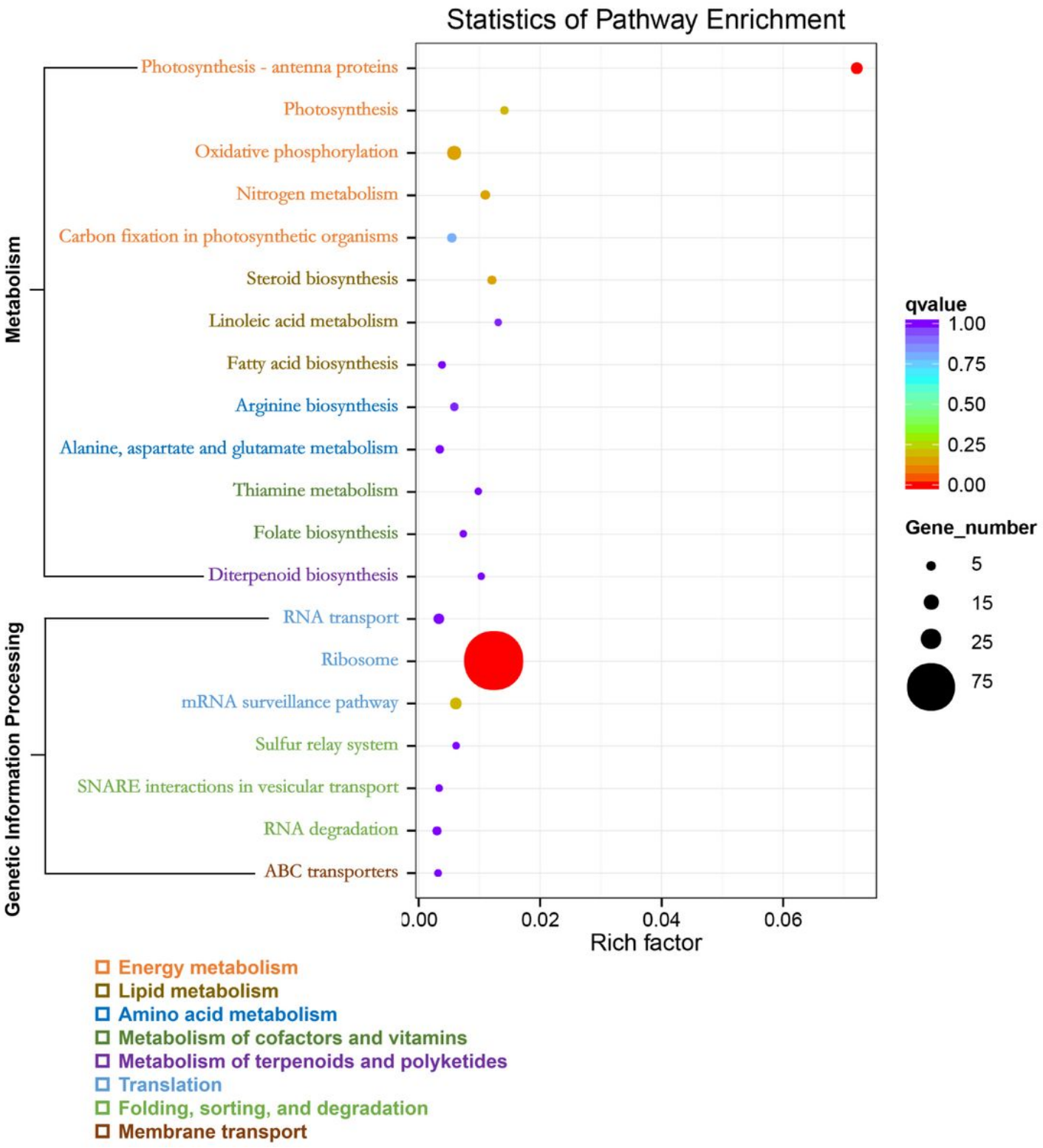


Figure 9

KEGG analysis of differentially expressed downregulated genes in root cells of hyperaccumulating ecotype of *S. alfredii* treated with 5 or 100 μM Zn for 24 h. The abscissa indicates the enrichment factor; the size indicates the number of genes; the color indicates the significance, the redder the color indicates the more significant the degree of enrichment; the ordinate indicates the metabolic pathway with the higher degree of enrichment; and the annotation color is classified according to the pathway.

Based on the transcriptome analysis, we further screened key gene resources (Fig. 10). The upregulated DEGs were associated with germin-like protein, auxin response factor, sugar transport protein, tryptophan metabolism, aminotransferase-related family protein, ammonium transporter, and urea active transporter. Downregulated DEGs were associated with wall-associated receptor kinase, serine/threonine protein kinase, polyamine oxidase, mitogen-activated protein kinase kinase, and serine/arginine-rich protein.

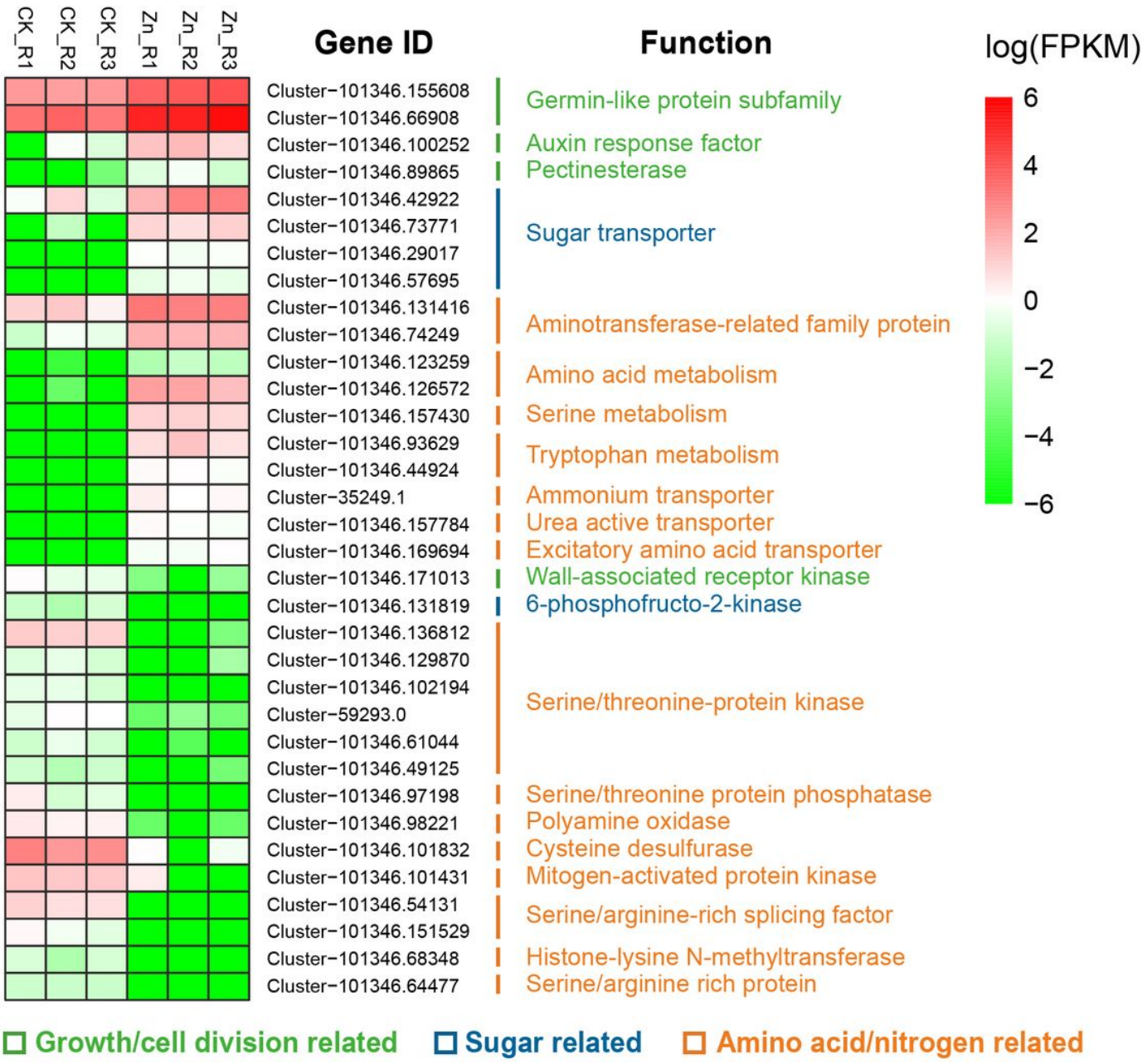


Figure 10

Expression profiles of the differentially expressed genes predicted to encode proteins which may be related to the growth of root cells of hyperaccumulating ecotype of *S. alfredii* treated with 5 or 100 μM Zn for 24 h. Relative expression was calculated using the log(FPKM) ratio.

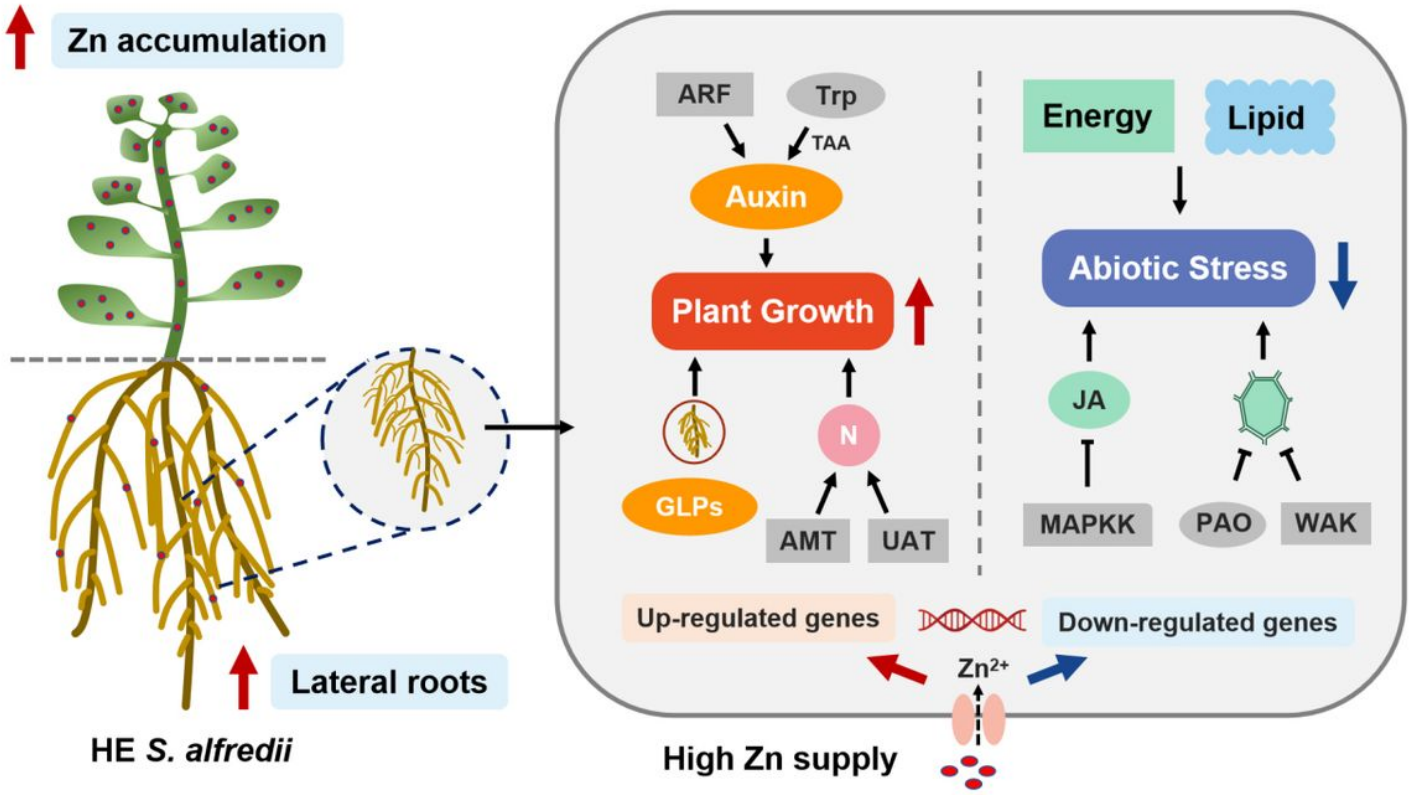


Figure 11

The mechanism involved in the positive effects of high zinc (Zn) on the growth of hyperaccumulating ecotype of *S. alfredii*. ARF, Auxin response factor; Trp, Tryptophan metabolism; AMT, Ammonium transporter; UAT, Urea active transporter; N, Nitrogen; GLPs, Germin-like protein subfamily; JA, Lateral root; MAPKK, Mitogen-activated protein kinase kinase; PAO, Polyamine oxidase; WAK, Wall-associated receptor kinase.